



HAL
open science

Finite element modeling of locally nonlinear infinite periodic structures using time-domain absorbing boundary conditions

D Duhamel, Jean-mathieu Mencik

► **To cite this version:**

D Duhamel, Jean-mathieu Mencik. Finite element modeling of locally nonlinear infinite periodic structures using time-domain absorbing boundary conditions. International Conference on Noise and Vibration Engineering (ISMA 2022), Sep 2022, Louvain, Belgium. 13 p. hal-03992804

HAL Id: hal-03992804

<https://hal.science/hal-03992804>

Submitted on 16 Feb 2023

HAL is a multi-disciplinary open access archive for the deposit and dissemination of scientific research documents, whether they are published or not. The documents may come from teaching and research institutions in France or abroad, or from public or private research centers.

L'archive ouverte pluridisciplinaire **HAL**, est destinée au dépôt et à la diffusion de documents scientifiques de niveau recherche, publiés ou non, émanant des établissements d'enseignement et de recherche français ou étrangers, des laboratoires publics ou privés.

Finite element modeling of locally nonlinear infinite periodic structures using time-domain absorbing boundary conditions

D. Duhamel¹, J.-M. Mencik²

¹ Ecole des Ponts ParisTech, Laboratoire Navier, ENPC/UGE/CNRS,
6 et 8 Avenue Blaise Pascal, Cité Descartes, Champs-sur-Marne, 77455 Marne La Vallée Cedex 2, France
e-mail: denis.duhamel@enpc.fr

² INSA Centre Val de Loire, Université d'Orléans, Université de Tours, LaMé,
3 Rue de la Chocolaterie, 41000 Blois, France
e-mail: jean-mathieu.mencik@insa-cvl.fr

Abstract

A finite element-based approach is proposed to compute the time response of infinite periodic structures with local nonlinearities. Under the assumption that the excitation sources and the nonlinear effects are localized, an infinite periodic structure can be modeled as a finite one with two left and right semi-infinite linear parts which are described via appropriate absorbing boundary conditions (BCs) formulated in the time domain using the wave finite element (WFE) method as recently proposed by the authors in [1]. The formulation of the absorbing BCs involves the usual vectors of displacements, velocities and accelerations, as well as vectors of supplementary variables. In this way, a classical second-order time differential equation for a nonlinear finite periodic structure with absorbing BCs can be formulated and integrated into a Newmark's algorithm for the temporal variable and a Newton Raphson's algorithm for the nonlinear equations. Numerical experiments are proposed which highlight the relevance of the approach for several types and levels of nonlinearities.

1 Introduction

The time response of infinite straight periodic structures with local nonlinearities is addressed. Such structures are usually made up of cells/substructures of arbitrary shapes (e.g., 2D substructures) and are broadly encountered in many engineering fields. Typical applications may concern railway tracks under dynamic loadings (trains) which are likely to induce a nonlinear behavior of the pad and the foundation, or metamaterial structures like beams with resonant devices which, when subjected to fast loadings of high amplitudes (impacts, shocks), are likely to be locally nonlinear. Under the assumption that the excitation sources and the nonlinear effects are localized, such infinite periodic structures can be modeled as a finite one with left and right absorbing BCs. Thus, the problem turns out to be the time-domain finite element (FE) analysis of a nonlinear finite periodic structure with absorbing BCs.

A formulation of absorbing BCs for linear periodic structures in the time domain has been recently proposed in [1] and is extended here to the study of locally nonlinear periodic ones. The procedure invokes the WFE method which is well suited for the modeling of periodic structures [2, 3, 4, 5, 6, 7, 8, 9, 10, 11, 12, 13, 14, 15]. In the WFE framework, absorbing BCs can be straightforwardly expressed in the frequency domain in terms of impedance matrices. These are obtained by analyzing the propagation of waves in structures and, as such, are accurate and constitute good alternatives to the usual techniques like the perfectly matched layer (PML) method [16, 17, 18, 19]. The strategy to express the absorbing BCs in the time domain can be summarized as follows:

1. Estimating the WFE impedance matrices via rational functions expressed in terms of identified poles

and associated residues;

2. Expressing the resulting absorbing BCs in terms of polynomials of the frequency $i\omega$ up to the order 2 using vectors of supplementary variables;
3. Expressing these polynomials in the time domain in order to obtain a classical dynamic equation with associated mass, damping and stiffness matrices.

Following the FE procedure, a global matrix system for a nonlinear finite periodic structure subjected to absorbing BCs can be proposed which involves the usual vectors of displacements, velocities and accelerations, and the vectors of supplementary variables. This yields a second-order time differential equation which can be integrated into a Newmark's algorithm for the temporal variable and a Newton Raphson's algorithm for the nonlinear equations.

The rest of the paper is organized as follows. In Sec. 2, some basics of the WFE method are given. In Sec. 3, the strategy for expressing the absorbing BCs of a periodic structure in the time domain is detailed; also, the nonlinear second-order differential equation for a nonlinear finite periodic structure with absorbing BCs is formulated. In Sec. 4, the strategy for solving the nonlinear equation of the structure with absorbing BCs is presented. Finally, in Sec. 5, numerical experiments are carried out concerning periodic structures made of nonlinear materials.

2 WFE method

The WFE method is a numerical approach to predict the propagation of waves in 1D periodic (linear) structures [3, 5, 20]. An infinite 1D structure composed of identical substructures and subjected to harmonic disturbance $e^{i\omega t}$ is shown in Fig. 1. Here, the FE models and FE meshes of the substructures are supposed to be similar, which means that they have the same mass, damping and stiffness matrices \mathbf{M} , \mathbf{C} and \mathbf{K} . The related dynamic equilibrium equation, for a substructure s , is given by:

$$\mathbf{D}\mathbf{q}^s = \mathbf{F}^s, \quad (1)$$

where \mathbf{q}^s and \mathbf{F}^s are the displacement and force vectors, respectively; also, \mathbf{D} is the dynamic stiffness matrix (similar for all the substructures) expressed by $\mathbf{D} = -\omega^2\mathbf{M} + i\omega\mathbf{C} + \mathbf{K}$.

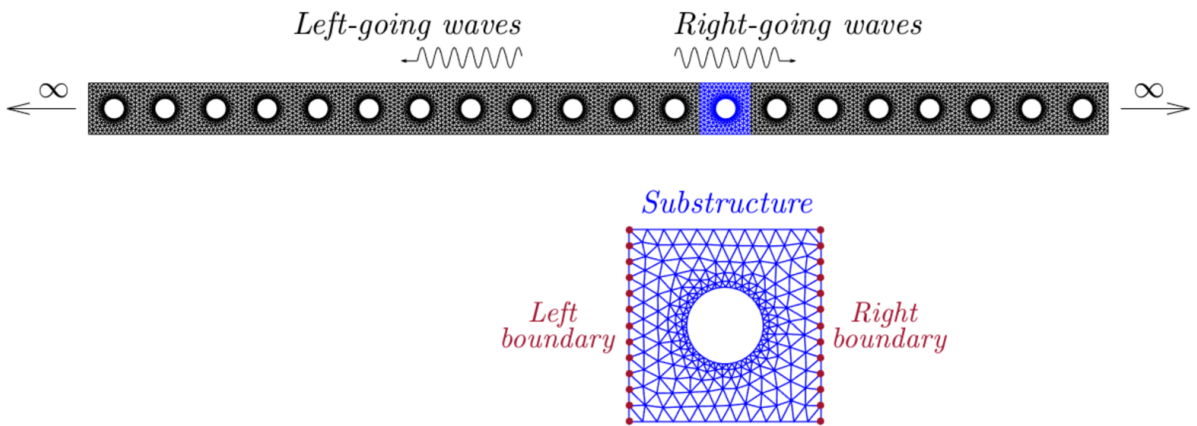


Figure 1: Periodic structure of infinite length, and FE mesh of a substructure.

The FE mesh of a substructure is shown in Fig. 1, and involves left (L) and right (R) boundaries with the same number n of degrees of freedom (DOFs) where coupling conditions with the other substructures are taken into account (coupling forces \mathbf{F}^s). After some manipulations, Eq. (1) can be rearranged into the following equation:

$$\mathbf{u}_R^s = \mathbf{S}\mathbf{u}_L^s, \quad (2)$$

where \mathbf{u}_R^s and \mathbf{u}_L^s are $2n \times 1$ state vectors expressed by:

$$\mathbf{u}_R^s = \begin{bmatrix} \mathbf{q}_R^s \\ \mathbf{F}_R^s \end{bmatrix}, \quad \mathbf{u}_L^s = \begin{bmatrix} \mathbf{q}_L^s \\ -\mathbf{F}_L^s \end{bmatrix}. \quad (3)$$

Also, \mathbf{S} is a $2n \times 2n$ symplectic matrix expressed by:

$$\mathbf{S} = \left[\begin{array}{c|c} -(\mathbf{D}_{LR}^*)^{-1}\mathbf{D}_{LL}^* & -(\mathbf{D}_{LR}^*)^{-1} \\ \hline \mathbf{D}_{RL}^* - \mathbf{D}_{RR}^*(\mathbf{D}_{LR}^*)^{-1}\mathbf{D}_{LL}^* & -\mathbf{D}_{RR}^*(\mathbf{D}_{LR}^*)^{-1} \end{array} \right], \quad (4)$$

where \mathbf{D}^* is the condensed dynamic stiffness matrix [7]. Note that the coupling conditions between two substructures s and $s + 1$, or between two substructures $s - 1$ and s , write:

$$\mathbf{u}_R^s = \mathbf{u}_L^{s+1} \quad \text{or} \quad \mathbf{u}_R^{s-1} = \mathbf{u}_L^s. \quad (5)$$

Then, from Eq. (2), the following transfer relations between two consecutive substructures can be obtained:

$$\mathbf{u}_L^{s+1} = \mathbf{S}\mathbf{u}_L^s \quad \text{or} \quad \mathbf{u}_R^s = \mathbf{S}\mathbf{u}_R^{s-1}, \quad (6)$$

where \mathbf{S} has the meaning of a transfer matrix. Since \mathbf{S} is symplectic, it has paired eigensolutions (μ_j, ϕ_j) and $(\mu_j^* = 1/\mu_j, \phi_j^*)$ with $|\mu_j| < 1$ (see [4] for further details about the computation of the eigensolutions of \mathbf{S}). Here, the eigenvalues of \mathbf{S} – namely, μ_j and μ_j^* – represent wave parameters defined as $\mu_j = e^{-ik_j d}$ and $\mu_j^* = e^{ik_j d}$ (k_j and d being the wavenumbers and the substructure length, respectively); also, the eigenvectors ϕ_j and ϕ_j^* represent wave shape vectors for the waves traveling to the right and left directions of the periodic structure, respectively. These are vectors of size $2n \times 1$ and are expressed as follows:

$$\phi_j = \begin{bmatrix} \phi_{qj} \\ \phi_{Fj} \end{bmatrix}, \quad \phi_j^* = \begin{bmatrix} \phi_{qj}^* \\ \phi_{Fj}^* \end{bmatrix}, \quad (7)$$

where ϕ_{qj} and ϕ_{qj}^* (resp. ϕ_{Fj} and ϕ_{Fj}^*) are $n \times 1$ vectors involving displacement (resp. force) components. The related $n \times n$ matrices of wave shapes – namely, Φ_q , Φ_q^* , Φ_F and Φ_F^* – are given by:

$$\Phi_q = [\phi_{q1} \cdots \phi_{qn}] \quad , \quad \Phi_q^* = [\phi_{q1}^* \cdots \phi_{qn}^*] \quad , \quad \Phi_F = [\phi_{F1} \cdots \phi_{Fn}] \quad , \quad \Phi_F^* = [\phi_{F1}^* \cdots \phi_{Fn}^*]. \quad (8)$$

3 Absorbing BCs

The analysis of a locally nonlinear infinite periodic structure can be undertaken by considering a periodic structure of finite length (N substructures) containing nonlinear effects and time dependent forces, and enclosed between two linear semi-infinite periodic structures which are described in terms of absorbing BCs. A nonlinear periodic structure with a finite number N of substructures and subjected to time-dependent forces (vector $\mathbf{F}(t)$) is shown in Fig. 2.

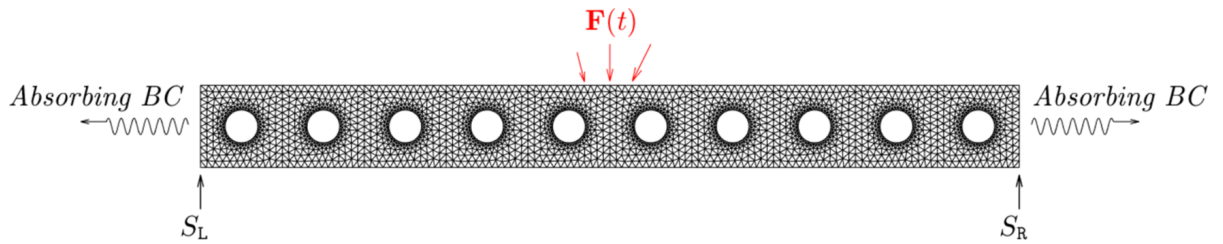


Figure 2: Nonlinear periodic structure with N substructures subjected to time-dependent forces and absorbing BCs.

The methodology to express the absorbing BCs of the nonlinear periodic structure in the time domain can

be summarized as follows [1]. The idea is that, far from the nonlinearities and the excitation sources, the structure is linear and is weakly subjected to evanescent/complex fields emanating from singularities. First, the impedance matrices (frequency domain) at the left (L) and right (R) ends of the periodic structure (N substructures) are estimated via the WFE method as follows:

$$\mathbf{Z}_L = -\Phi_F^*(\Phi_q^*)^{-1}, \quad \mathbf{Z}_R = \Phi_F(\Phi_q)^{-1}. \quad (9)$$

These impedance matrices are derived by expressing the displacement/force vectors in terms of wave shape vectors [4], and by cancelling the amplitudes for the waves emanating from infinity. The second step of the proposed approach is to estimate the impedance matrices \mathbf{Z}_L and \mathbf{Z}_R via rational approximations:

$$\mathbf{Z}_L = \sum_{k=1}^Q 2 \frac{i\omega \Re\{\mathbf{R}_{L(2k)}\} - \Re\{\overline{p_{L(2k)}} \mathbf{R}_{L(2k)}\}}{-\omega^2 - 2i\omega \Re\{p_{L(2k)}\} + |p_{L(2k)}|^2} + \sum_{k=2Q+1}^P \frac{\mathbf{R}_{Lk}}{i\omega - p_{Lk}} + \mathbf{K}_L, \quad (10)$$

$$\mathbf{Z}_R = \sum_{k=1}^Q 2 \frac{i\omega \Re\{\mathbf{R}_{R(2k)}\} - \Re\{\overline{p_{R(2k)}} \mathbf{R}_{R(2k)}\}}{-\omega^2 - 2i\omega \Re\{p_{R(2k)}\} + |p_{R(2k)}|^2} + \sum_{k=2Q+1}^P \frac{\mathbf{R}_{Rk}}{i\omega - p_{Rk}} + \mathbf{K}_R, \quad (11)$$

where (p_{Lk}, p_{Rk}) and $(\mathbf{R}_{Lk}, \mathbf{R}_{Rk})$ denote poles and matrices of residues ($k = 1, \dots, P$), respectively. These usually appear in conjugate pairs, e.g., Q pairs. Note that the absorbing BCs at the left and right end of the periodic structure are expressed in the frequency domain as $\mathbf{F}_L = \mathbf{Z}_L \mathbf{q}_L$ and $\mathbf{F}_R = \mathbf{Z}_R \mathbf{q}_R$. By considering vectors of supplementary variables \mathbf{X}_{Lk} and \mathbf{X}_{Rk} in Eqs. (10) and (11), it can be shown that the absorbing BCs can be alternatively written as follows:

$$\mathbf{F}_L = \sum_{k=1}^Q 2 (i\omega \Re\{\mathbf{R}_{L(2k)}\} - \Re\{\overline{p_{L(2k)}} \mathbf{R}_{L(2k)}\}) \mathbf{X}_{Lk} + \sum_{k=2Q+1}^P \mathbf{R}_{Lk}(i\omega) \mathbf{X}_{L(k-Q)} + \mathbf{K}_L \mathbf{q}_L, \quad (12)$$

$$\mathbf{F}_R = \sum_{k=1}^Q 2 (i\omega \Re\{\mathbf{R}_{R(2k)}\} - \Re\{\overline{p_{R(2k)}} \mathbf{R}_{R(2k)}\}) \mathbf{X}_{Rk} + \sum_{k=2Q+1}^P \mathbf{R}_{Rk}(i\omega) \mathbf{X}_{R(k-Q)} + \mathbf{K}_R \mathbf{q}_R, \quad (13)$$

where:

$$(-\omega^2 - 2i\omega \Re\{p_{L(2k)}\} + |p_{L(2k)}|^2) \mathbf{X}_{Lk} = \mathbf{q}_L \quad \text{for } k = 1, \dots, Q, \quad (14)$$

$$(-\omega^2 - 2i\omega \Re\{p_{R(2k)}\} + |p_{R(2k)}|^2) \mathbf{X}_{Rk} = \mathbf{q}_R \quad \text{for } k = 1, \dots, Q, \quad (15)$$

$$(-\omega^2 - i\omega p_{Lk}) \mathbf{X}_{L(k-Q)} = \mathbf{q}_L \quad \text{for } k = (2Q+1), \dots, P, \quad (16)$$

$$(-\omega^2 - i\omega p_{Rk}) \mathbf{X}_{R(k-Q)} = \mathbf{q}_R \quad \text{for } k = (2Q+1), \dots, P. \quad (17)$$

In Eqs. (12) and (13), the force vectors are described in terms of polynomials of $i\omega$ of order 1. On the other hand, Eqs. (14)-(17) express the relations between the displacement vectors and the vectors of supplementary variables, which are described in terms of polynomials of $i\omega$ too (up to order 2). By separating the terms of identical powers of $i\omega$ in Eqs. (12)-(17), and by invoking the classical time-frequency transforms $\mathbf{q}(\omega) \rightarrow \mathbf{q}(t)$, $i\omega \mathbf{q} \rightarrow \dot{\mathbf{q}}$, $-\omega^2 \mathbf{q} \rightarrow \ddot{\mathbf{q}}$ and $\mathbf{X}(\omega) \rightarrow \mathbf{X}(t)$, $i\omega \mathbf{X} \rightarrow \dot{\mathbf{X}}$, $-\omega^2 \mathbf{X} \rightarrow \ddot{\mathbf{X}}$ (where dot and double-dot notations mean single and double time derivatives, respectively), the following second-order time differential equations are obtained [1]:

$$\mathbb{M}_L \begin{bmatrix} \ddot{\mathbf{q}}_L \\ \ddot{\mathbf{X}}_L \end{bmatrix} + \mathbb{C}_L \begin{bmatrix} \dot{\mathbf{q}}_L \\ \dot{\mathbf{X}}_L \end{bmatrix} + \mathbb{K}_L \begin{bmatrix} \mathbf{q}_L \\ \mathbf{X}_L \end{bmatrix} = \begin{bmatrix} \mathbf{F}_L \\ \mathbf{0} \end{bmatrix}, \quad (18)$$

$$\mathbb{M}_R \begin{bmatrix} \ddot{\mathbf{q}}_R \\ \ddot{\mathbf{X}}_R \end{bmatrix} + \mathbb{C}_R \begin{bmatrix} \dot{\mathbf{q}}_R \\ \dot{\mathbf{X}}_R \end{bmatrix} + \mathbb{K}_R \begin{bmatrix} \mathbf{q}_R \\ \mathbf{X}_R \end{bmatrix} = \begin{bmatrix} \mathbf{F}_R \\ \mathbf{0} \end{bmatrix}, \quad (19)$$

where \mathbf{X}_L and \mathbf{X}_R are vectors built from \mathbf{X}_{Lk} and \mathbf{X}_{Rk} . Eqs. (18) and (19) can be simply integrated into the FE model of the nonlinear periodic structure (N substructures). Indeed, the FE discretization of the nonlinear

structure can be classically expressed by:

$$\mathbf{M}\ddot{\mathbf{q}} + \mathbf{C}\dot{\mathbf{q}} + \mathbf{F}^{\text{NL}}(\mathbf{q}) = \mathbf{F}, \quad (20)$$

where \mathbf{M} and \mathbf{C} here represent the mass and damping matrices of the structure. Also, \mathbf{q} and \mathbf{F} are the vectors of displacements and external forces expressed by:

$$\mathbf{q} = \mathbf{q}(t) = \begin{bmatrix} \mathbf{q}_I(t) \\ \mathbf{q}_L(t) \\ \mathbf{q}_R(t) \end{bmatrix}, \quad \mathbf{F} = \mathbf{F}(t) = \begin{bmatrix} \mathbf{F}_I(t) \\ \mathbf{F}_L(t) \\ \mathbf{F}_R(t) \end{bmatrix}, \quad (21)$$

where $\mathbf{q}_I(t)$ and $\mathbf{F}_I(t)$ denote the displacement vector and the force vector – i.e., the time loading applied to the structure – for the internal DOFs (between the left and right ends). Also, in Eq. (20), $\mathbf{F}^{\text{NL}}(\mathbf{q})$ is a nonlinear vector-valued function whose expression relies upon the type of nonlinearities considered. By considering the absorbing BCs, Eqs. (18) and (19), the dynamic equation of the nonlinear periodic structure, Eq. (20), can be rewritten as follows:

$$\mathbf{M}_{\text{tot}}\ddot{\mathbf{y}} + \mathbf{C}_{\text{tot}}\dot{\mathbf{y}} + \mathbf{F}_{\text{tot}}^{\text{NL}}(\mathbf{y}) = \mathbf{F}_{\text{tot}}, \quad (22)$$

where

$$\mathbf{y} = \mathbf{y}(t) = \begin{bmatrix} \mathbf{q}_I(t) \\ \mathbf{q}_L(t) \\ \mathbf{q}_R(t) \\ \mathbf{X}_L(t) \\ \mathbf{X}_R(t) \end{bmatrix}, \quad \mathbf{F}_{\text{tot}} = \mathbf{F}_{\text{tot}}(t) = \begin{bmatrix} \mathbf{F}_I(t) \\ \mathbf{0} \\ \mathbf{0} \\ \mathbf{0} \\ \mathbf{0} \end{bmatrix}. \quad (23)$$

In Eq. (22), \mathbf{M}_{tot} , \mathbf{C}_{tot} and $\mathbf{F}_{\text{tot}}^{\text{NL}}(\mathbf{y})$ are matrices/vector which are built by expressing \mathbf{F}_L and \mathbf{F}_R in Eq. (21) via Eqs. (18) and (19).

4 Solution procedure

Eq. (22) is a nonlinear second-order time differential equation which can be solved with the Newmark method. Then, let us denote by \mathbf{y}^n and \mathbf{y}^{n+1} two solutions of Eq. (22) at two consecutive time steps t_n and t_{n+1} (time step Δt). The Newmark algorithm can be detailed as follows:

$$\dot{\mathbf{y}}^{n+1} = \dot{\mathbf{y}}^n + (1 - \gamma)\Delta t \ddot{\mathbf{y}}^n + \gamma\Delta t \ddot{\mathbf{y}}^{n+1} \quad (24)$$

$$\mathbf{y}^{n+1} = \mathbf{y}^n + \Delta t \dot{\mathbf{y}}^n + \frac{\Delta t^2}{2} ((1 - 2\beta)\ddot{\mathbf{y}}^n + 2\beta\ddot{\mathbf{y}}^{n+1}) \quad (25)$$

$$\mathbf{M}_{\text{tot}}\ddot{\mathbf{y}}^{n+1} + \mathbf{C}_{\text{tot}}\dot{\mathbf{y}}^{n+1} + \mathbf{F}_{\text{tot}}^{\text{NL}}(\mathbf{y}^{n+1}) = \mathbf{F}_{\text{tot}}(t_{n+1}) \quad (26)$$

Here, γ and β represent the Newmark parameters which are chosen as $\gamma = 1/2$ and $\beta = 1/4$ in accordance with the average constant acceleration rule. Eq. (26) is nonlinear and must be solved at each time step. Here, the Newton-Raphson algorithm is used. This first consists in introducing the following predictors defined at time t_{n+1} and depending on the solutions at time t_n :

$$\tilde{\mathbf{y}}^{n+1} = \mathbf{y}^n + \Delta t \dot{\mathbf{y}}^n + \left(\frac{1}{2} - \beta\right)\Delta t^2 \ddot{\mathbf{y}}^n \quad (27)$$

$$\dot{\tilde{\mathbf{y}}}^{n+1} = \dot{\mathbf{y}}^n + (1 - \gamma)\Delta t \ddot{\mathbf{y}}^n \quad (28)$$

Then the following initial guesses at time t_{n+1} , for the Newton-Raphson iteration step $k = 0$, can be proposed:

$$\mathbf{y}_0^{n+1} = \tilde{\mathbf{y}}^{n+1} \quad (29)$$

$$\dot{\mathbf{y}}_0^{n+1} = \dot{\tilde{\mathbf{y}}}^{n+1} \quad (30)$$

$$\mathbf{R}_0^{n+1} = \mathbf{F}_{\text{tot}}(t_{n+1}) - \mathbf{C}_{\text{tot}}\dot{\mathbf{y}}_0^{n+1} - \mathbf{F}_{\text{tot}}^{\text{NL}}(\mathbf{y}_0^{n+1}) \quad (31)$$

The Newton-Raphson iteration scheme can be detailed as follows (step k):

$$\Delta\ddot{\mathbf{y}}_{k+1}^{n+1} = (\mathbf{M}_{\text{tot}} + \gamma\Delta t\mathbf{C}_{\text{tot}} + \beta\Delta t^2\mathcal{K}_k^{n+1})^{-1} \mathbf{R}_k^{n+1} \quad (32)$$

$$\ddot{\mathbf{y}}_{k+1}^{n+1} = \ddot{\mathbf{y}}_k^{n+1} + \Delta\ddot{\mathbf{y}}_{k+1}^{n+1} \quad (33)$$

$$\dot{\mathbf{y}}_{k+1}^{n+1} = \dot{\mathbf{y}}_k^{n+1} + \gamma\Delta t \Delta\ddot{\mathbf{y}}_{k+1}^{n+1} \quad (34)$$

$$\mathbf{y}_{k+1}^{n+1} = \mathbf{y}_k^{n+1} + \beta\Delta t^2 \Delta\ddot{\mathbf{y}}_{k+1}^{n+1} \quad (35)$$

$$\mathbf{R}_{k+1}^{n+1} = \mathbf{F}(t_{n+1}) - \mathbf{M}_{\text{tot}}\ddot{\mathbf{y}}_{k+1}^{n+1} - \mathbf{C}_{\text{tot}}\dot{\mathbf{y}}_{k+1}^{n+1} - \mathbf{F}_{\text{tot}}^{\text{NL}}(\mathbf{y}_{k+1}^{n+1}) \quad (36)$$

The algorithm iterates until the norm of the residue $\|\mathbf{R}_{k+1}^{n+1}\|$ becomes sufficiently small. The final value of k is denoted by k_{n+1} and yields the solutions of Eq. (22) at time t_{n+1} :

$$\mathbf{y}^{n+1} = \mathbf{y}_{k_{n+1}}^{n+1} \quad (37)$$

$$\dot{\mathbf{y}}^{n+1} = \dot{\mathbf{y}}_{k_{n+1}}^{n+1} \quad (38)$$

$$\ddot{\mathbf{y}}^{n+1} = \ddot{\mathbf{y}}_{k_{n+1}}^{n+1} \quad (39)$$

In Eq. (32), \mathcal{K}_k^{n+1} is the tangent stiffness matrix which is given by:

$$\mathcal{K}_k^{n+1} = \frac{\partial \mathbf{F}_{\text{tot}}^{\text{NL}}}{\partial \mathbf{y}}(\mathbf{y}_k^{n+1}). \quad (40)$$

Also, in Eq. (36), $\mathbf{F}_{\text{tot}}^{\text{NL}}(\mathbf{y}_{k+1}^{n+1})$ is the nonlinear term which can be evaluated from the stress tensor at the Gauss points of the elements of the structure. The stress tensor is obtained from the constitutive relations which, for hyperelastic materials with an elastic potential $\Psi(\mathbf{F})$, are such that the first Piola–Kirchhoff stress tensor (namely, \mathbf{P}) verifies:

$$\mathbf{P} = \frac{\partial \Psi}{\partial \mathbf{F}}, \quad (41)$$

where \mathbf{F} is the gradient of the transformation. In this framework, the Cauchy stress tensor is given by:

$$\boldsymbol{\sigma} = \frac{1}{J} \frac{\partial \Psi}{\partial \mathbf{F}} \cdot \mathbf{F}^T, \quad (42)$$

where $J = \det(\mathbf{F})$.

5 Numerical results

Numerical experiments are carried out concerning periodic structures with two types of nonlinearities (Neo-Hookean material and Mooney-Rivlin material). For each case, the time response of the infinite structure is estimated using the proposed approach and compared with a reference FE solution. The reference solution involves computing the time response for a structure with many substructures which is supposed to behave like an infinite one. On the other hand, the proposed approach involves considering a structure with a small number of substructures, and adding absorbing BCs via the WFE method, see Sec. 2 and Sec. 3. Concerning the numerical methodology, the wave parameters μ_j and μ_j^* , the wave shape vectors ϕ_j and ϕ_j^* , the impedance matrices \mathbf{Z}_L and \mathbf{Z}_R , and the matrices $\mathbf{M}_L, \mathbf{M}_R, \mathbf{C}_L, \mathbf{C}_R, \mathbf{K}_L, \mathbf{K}_R$ in Eqs. (18) and (19) are obtained using Matlab and Gmsh (substructure FE mesh). Afterwards, the matrices in Eqs. (18) and (19)

are implemented on FEniCS to model a nonlinear periodic structure with time-domain absorbing BCs. This allows an easy consideration of the nonlinear part of a structure from an elastic potential. Several examples are presented below.

5.1 Uniform substructures with a homogeneous Neo-Hookean material

Let us consider a locally nonlinear infinite structure with uniform substructures of size $L_x \times L_y = 2 \times 2 \text{ m}^2$ in the (x, y) -plane as shown in Fig. 3. 2D substructures of thickness $e = 0.005 \text{ m}$ which are meshed with plane stress triangular elements are considered. The linear material properties considered here are: Young's modulus $E = 70 \times 10^9 \text{ Pa}$, Poisson's ratio $\nu = 0.35$, density $\rho = 2700 \text{ kg/m}^3$. The whole structure is supposed to lie on an elastic foundation (rigidity of $0.5 \times 10^7 \text{ N/m}$) which is modeled by means of equally-spaced identical linear springs at the bottom nodes of the FE mesh. Nonlinear effects are taken into account and are supposed to be restricted to a region encompassing 20 consecutive substructures in the center of which – i.e., for the two central substructures – a lineic harmonic force of magnitude $2 \times 10^7 \text{ N/m}$ and frequency 100 Hz – i.e., $2 \times 10^7 \cos(2\pi 100t) \text{ N/m}$ – is suddenly applied at $t = 0 \text{ s}$.

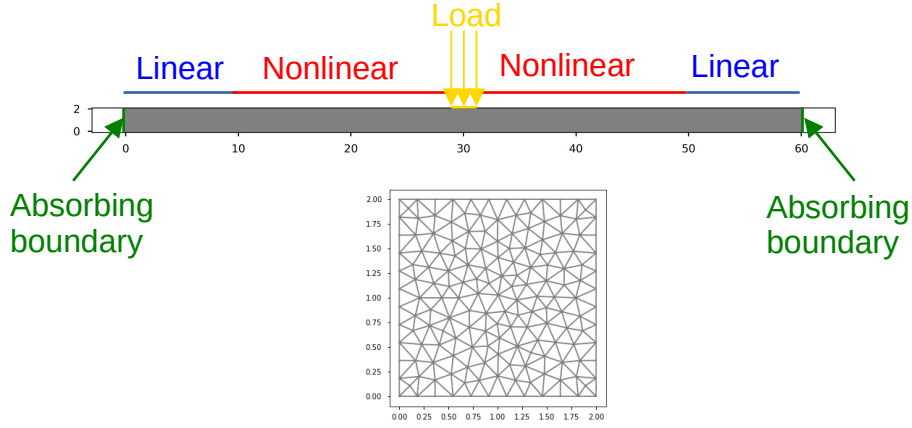


Figure 3: Schematic of a locally nonlinear structure with uniform substructures and absorbing BCs, and FE mesh of a substructure.

Within the framework of the proposed approach, a finite periodic structure with 30 substructures is considered which here concern the aforementioned 20 nonlinear substructures and 5 additional linear substructures on the left and right sides. Absorbing BCs at the left and right ends are obtained via the strategy proposed in Sec. 3.

For modeling the nonlinear substructures, a compressible Neo-Hookean material is considered with an elastic potential Ψ given by:

$$\Psi = \frac{\mu}{2}(I_c - 2) - \mu \ln(J) + \frac{\lambda}{2} \ln(J)^2, \quad (43)$$

where:

$$I_c = \text{Tr}(\mathbf{F}^T \mathbf{F}), \quad (44)$$

$$J = \det(\mathbf{F}). \quad (45)$$

Here, \mathbf{F} represents the gradient of the transformation. Also, $\lambda = 6.04 \times 10^{10} \text{ Pa}$ and $\mu = 2.60 \times 10^{10} \text{ Pa}$. These parameters are such that, for small strains, the behavior of the material is the same as the linear substructures.

The total simulation time is 0.1 s with a time step of $\Delta t = 5 \times 10^{-4} \text{ s}$. For computing the absorbing BCs, the WFE-based impedance matrices \mathbf{Z}_L and \mathbf{Z}_R are estimated between 5 Hz and 300 Hz using 1000 frequency points, and are then approximated via Eqs. (10) and (11) with 30 poles. The space variation of

the displacement modulus of the nonlinear structure at $t = 0.1$ s is shown in Fig. 4 where, for the sake of clarity, only 10 substructures are displayed. Also, the displacement solution for the equivalent purely linear structure is highlighted. These results show that, under high loading, nonlinear effects are present and provide displacement fields which cannot be predicted by the linear model. Besides the difference between the linear and nonlinear solutions can be further highlighted in Fig. 4, see bottom figure. Also, the space variations of the strain field ϵ_{xx} for the nonlinear and the linear cases, as well as the difference between the two solutions, can be computed as shown in Fig. 5. Again, the nonlinear solution appears to be significantly different from the linear one.

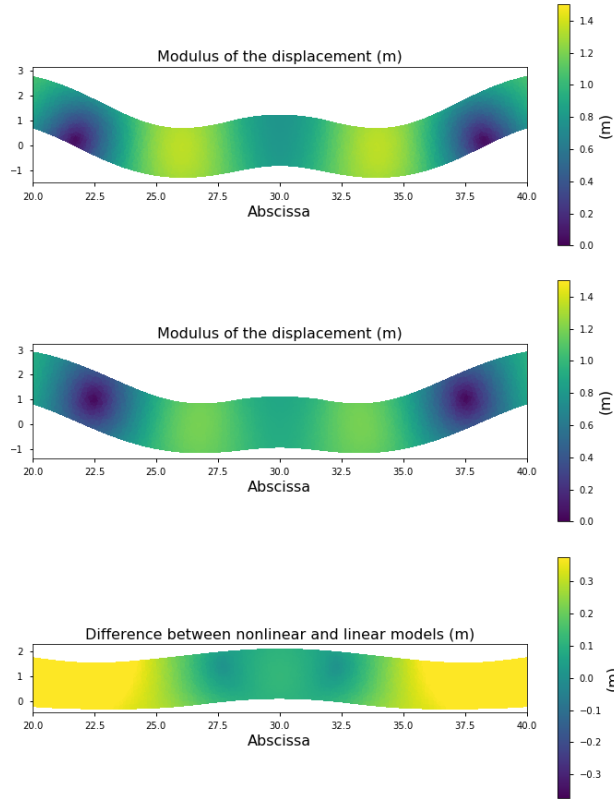


Figure 4: Modulus of the displacements for the nonlinear structure with a Neo-Hookean material (top) and the equivalent linear structure (middle); modulus of the difference in displacements between the two models (bottom).

Finally, Fig. 6 shows the time history for the x - and y -displacement components at point $(2L_x, L_y/2)$ (here, the origin of the (x, y) -plane corresponds to the center of the loaded area, see Fig. 3). Again, locally nonlinear and purely linear structures with absorbing BCs are considered. Also, for comparison purposes, reference solutions involving structures with a large number of substructures are analyzed (see comments at the beginning of Sec. 5). These reference structures are built from 300 substructures – i.e., 20 nonlinear or linear substructures with 140 extra linear substructures on each side – which are considered to prevent wave reflection effects from infinity within the time band analyzed. For each (nonlinear or linear) case, the proposed solution correctly agrees with the reference one over the whole time period. This fully validates the proposed approach. On the other hand, the difference between the nonlinear solution and the linear one is very clear regarding the x -displacement component, although less pronounced in the case of the y -displacement.

5.2 Substructures with holes and a homogeneous Mooney-Rivlin material

Let us consider now the case of a locally nonlinear infinite periodic structure involving square substructures with holes as shown in Fig. 7. 2D substructures under plane stress behavior, with global dimensions $L_x \times$

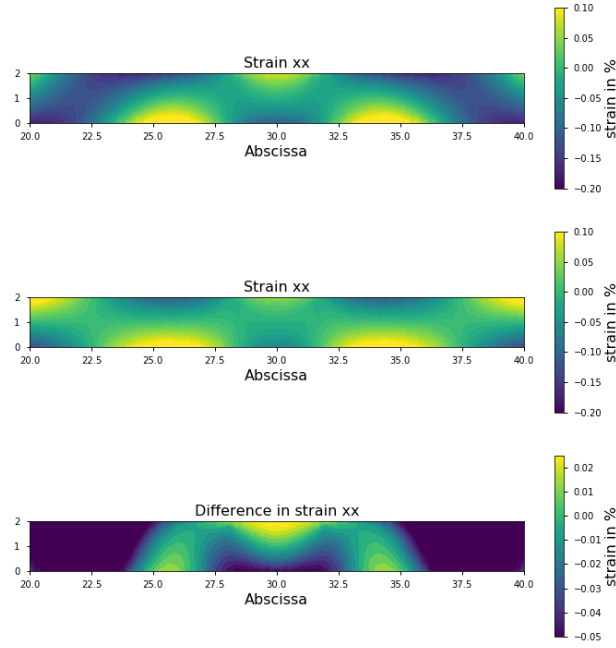


Figure 5: Modulus of the strains e_{xx} for the nonlinear structure with a Neo-Hookean material (top) and the equivalent linear structure (middle); modulus of the difference in strains between the two models (bottom).

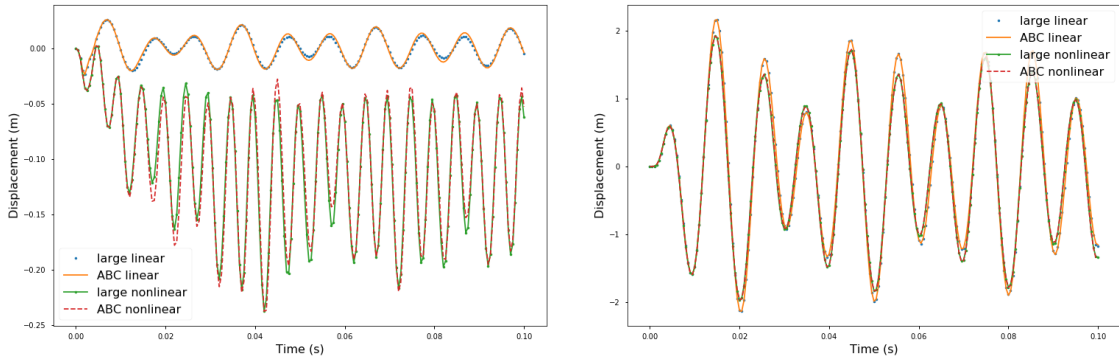


Figure 6: Time history for the x -displacement component (left) and the y -displacement component (right) of the nonlinear (Neo-Hookean material) and linear structures. Comparisons between the proposed solutions (ABC) and the reference ones (large).

$L_y = 2 \times 2 \text{ m}^2$ (thickness $e = 0.005 \text{ m}$) and a central hole of radius $R = 0.4 \text{ m}$, are considered. Again, the whole structure is supposed to lie on an elastic foundation (rigidity of $0.5 \times 10^7 \text{ N/m}$) and is subjected to a localized lineic force (magnitude of $2 \times 10^7 \text{ N/m}$, frequency of 100 Hz) in the same way as Sec. 5.1. Again, a finite periodic structure consisting of 20 nonlinear substructures and 5 linear substructures on the left and right sides is considered as shown in Fig. 3, where the material properties of the linear substructures are similar to those in Sec. 5.1.

In the present case, the nonlinear substructures are modeled using a compressible Mooney-Rivlin material with the following elastic potential:

$$\Psi = C_{10}(\bar{I}_1 - 2) + C_{01}(\bar{I}_2 - 2) + D(J - 1)^2. \quad (46)$$

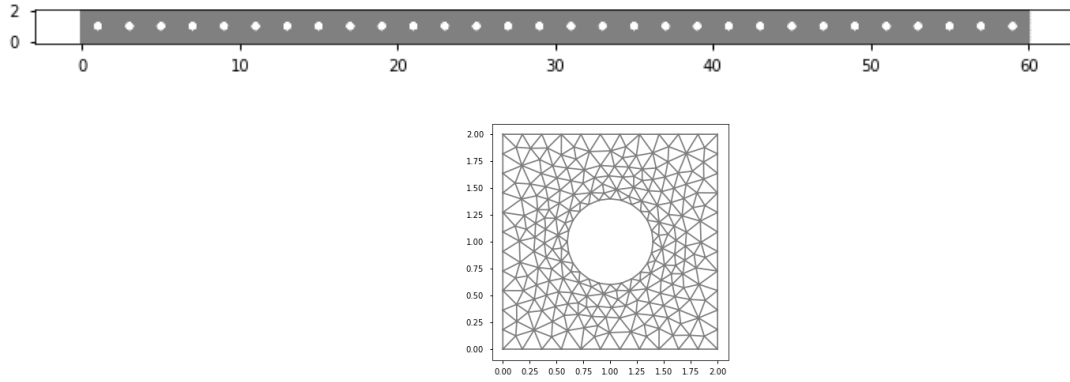


Figure 7: Schematic of a locally nonlinear periodic structure with heterogeneous substructures (squares with holes) and absorbing BCs, and FE mesh of a substructure.

Here:

$$\bar{I}_1 = \frac{1}{J^{2/3}}(\text{Tr}(\mathbf{B}) + 1), \quad (47)$$

$$\bar{I}_2 = \frac{1}{2J^{4/3}}((\text{Tr}(\mathbf{B}))^2 - \text{Tr}(\mathbf{B}\mathbf{B}) + 2\text{Tr}(\mathbf{B})), \quad (48)$$

$$\mathbf{B} = \mathbf{F}\mathbf{F}^T, \quad (49)$$

$$J = \det(\mathbf{F}), \quad (50)$$

where $C_{10} = 8.97 \times 10^9$ Pa, $C_{01} = 4.00 \times 10^9$ Pa and $D = 3.89 \times 10^{10}$ Pa. The implementation of this hyperelastic model on FEniCS is straightforward and does not required significant efforts, i.e., to move from the previous case to the present one. Indeed, the relevant parameter to change is the elastic potential.

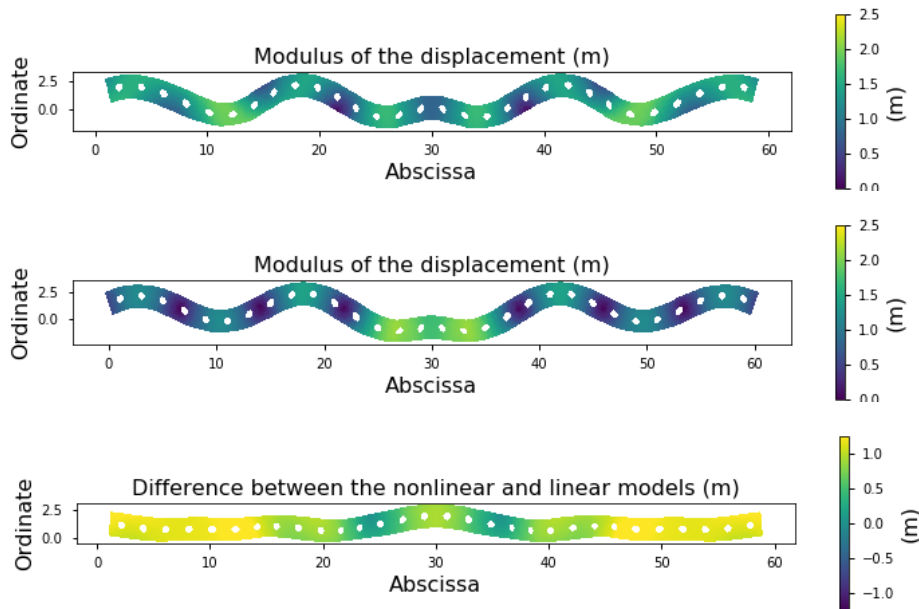


Figure 8: Modulus of the displacements for the nonlinear periodic structure with a Mooney-Rivlin material (top) and the equivalent linear periodic structure (middle); modulus of the difference in displacements between the two models (bottom).

For modeling the absorbing BCs of the finite periodic structure, the strategy proposed in Sec. 3 is used in the same way as Sec. 5.1. The displacement fields for the locally nonlinear structure and the equivalent purely linear one at $t = 0.1$ s, and the related difference, are shown in Fig. 8. Again, the nonlinear effects are highlighted in the sense that the magnitudes of the displacement fields issued from the nonlinear and linear models are significantly different in the vicinity of the excitation source. The analysis of the strain fields, not shown here, leads to similar conclusions, see Sec. 5.1.

Fig. 9 shows the time history for the x - and y -displacement components at point $(2L_x, L_y/2)$, in a similar way as in Sec. 5.1. Here, similar trends can be observed, i.e., the fact that overall the time response of the structure is strongly affected by the nonlinearities.

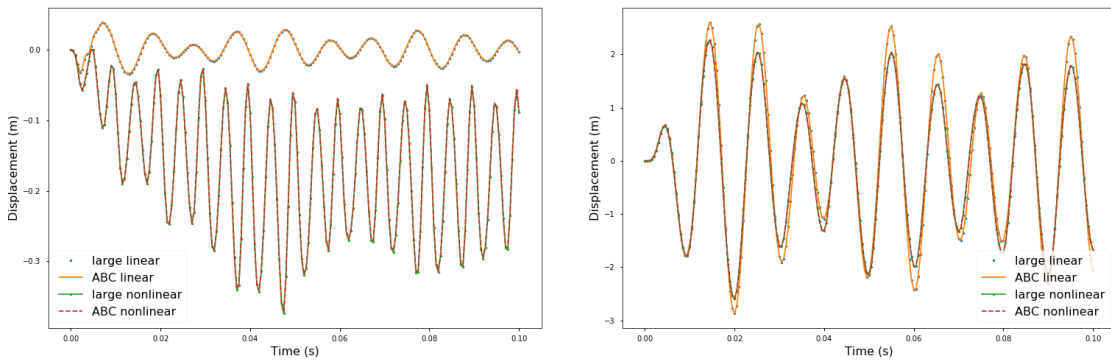


Figure 9: Time history for the x -displacement component (left) and the y -displacement component (right) of the nonlinear (Mooney-Rivlin material) and linear structures. Comparisons between the proposed solutions (ABC) and reference solutions (large).

Finally, a sensitivity analysis of the proposed approach can be proposed. The idea is to see whether the consideration of a periodic structure with 20 nonlinear substructures and 2×5 linear substructures, as in the present case, is relevant to approximate a nonlinear structure which should be totally described, in theory, with nonlinear substructures, i.e., 30 nonlinear substructures without linear ones. The underlying issue is to show that, far from the excitation sources, nonlinear substructures can be described from a linear model. Results are shown in Fig. 10. No significant differences can be detected. Besides this is the fact that the nonlinear behavior of the substructures, when they are considered close to the boundaries (absorbing BCs), does not affect the proposed approach as long as the nonlinearities are small in these regions.

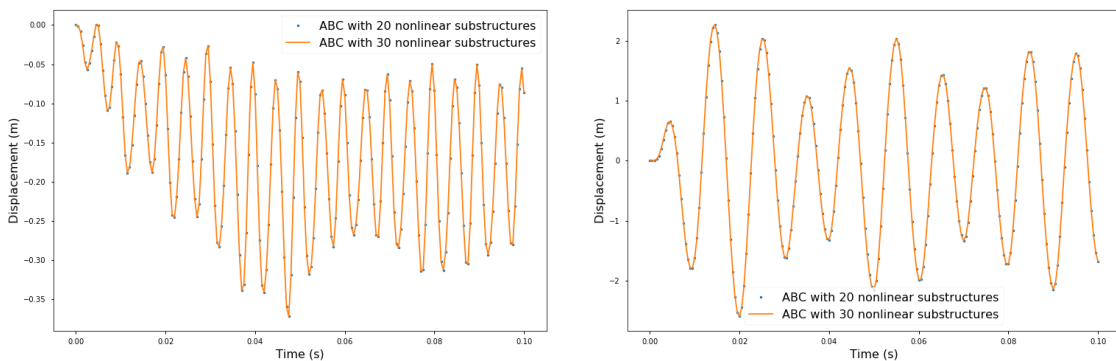


Figure 10: Time history for the x -displacement component (left) and the y -displacement component (right) of the nonlinear (Mooney-Rivlin material) and linear structures. Comparisons between a structure model with 20 nonlinear substructures (with 2×5 extra linear substructures) and a structure model with 30 nonlinear substructures (without linear substructures).

6 Conclusion

A finite element-based approach has been proposed for computing the time response of locally nonlinear infinite periodic structures. In this framework, an infinite periodic structure is described from a nonlinear periodic structure of finite length with appropriate absorbing BCs. Under the assumption that the boundaries of the finite structure are far enough from the excitation sources and the nonlinearities (about five substructures), the absorbing BCs can be expressed using the WFE method. The proposed absorbing BCs are formulated in the time domain using vectors of supplementary variables, and can be simply integrated into the FE model of a nonlinear periodic structure. Numerical results have been proposed concerning periodic structures with homogeneous substructures or more complex substructures subjected to several types of nonlinearities (Neo-Hookean and Mooney-Rivlin materials). For each case, the nonlinear behavior of the structure has been highlighted through comparisons with a linear analysis. Also, the accuracy of the proposed approach has been fully demonstrated. Follow-on works could include the analysis of locally nonlinear metamaterial structures, e.g., including resonant substructures with a nonlinear material.

References

- [1] D. Duhamel and J.-M. Mencik, "Time response analysis of periodic structures via wave-based absorbing boundary conditions," *European Journal of Mechanics - A/Solids*, vol. 91, p. 104418, 2022.
- [2] B. Mace, D. Duhamel, M. Brennan, and L. Hinke, "Finite element prediction of wave motion in structural waveguides," *Journal of the Acoustical Society of America*, vol. 117, pp. 2835–2843, 2005.
- [3] D. Duhamel, B. R. Mace, and M. J. Brennan, "Finite element analysis of the vibrations of waveguides and periodic structures," *Journal of Sound and Vibration*, vol. 294, no. 1-2, pp. 205–220, 2006.
- [4] J.-M. Mencik and D. Duhamel, "A wave-based model reduction technique for the description of the dynamic behavior of periodic structures involving arbitrary-shaped substructures and large-sized finite element models," *Finite Elements in Analysis and Design*, vol. 101, pp. 1–14, 2015.
- [5] J.-M. Mencik and M. N. Ichchou, "Multi-mode propagation and diffusion in structures through finite elements," *European Journal of Mechanics - A/Solids*, vol. 24, no. 5, pp. 877–898, 2005.
- [6] J.-M. Mencik and D. Duhamel, "A wave finite element-based approach for the modeling of periodic structures with local perturbations," *Finite Elements in Analysis and Design*, vol. 121, pp. 40 – 51, Nov. 2016.
- [7] J.-M. Mencik, "New advances in the forced response computation of periodic structures using the wave finite element (WFE) method," *Computational Mechanics*, vol. 54, no. 3, pp. 789–801, 2014.
- [8] J.-M. Mencik, "A model reduction strategy for computing the forced response of elastic waveguides using the wave finite element method," *Computer Methods in Applied Mechanics and Engineering*, vol. 229-232, pp. 68–86, 2012.
- [9] J.-M. Mencik, "A wave finite element approach for the analysis of periodic structures with cyclic symmetry in dynamic substructuring," *Journal of Sound and Vibration*, vol. 431, pp. 441–457, 2018.
- [10] M. N. Ichchou, J.-M. Mencik, and W. J. Zhou, "Wave finite elements for low and mid-frequency description of coupled structures with damage," *Computer Methods in Applied Mechanics and Engineering*, vol. 198, no. 15-16, pp. 1311–1326, 2009.
- [11] T. Hoang, D. Duhamel, and G. Foret, "Wave finite element method for waveguides and periodic structures subjected to arbitrary loads," *Finite Elements in Analysis and Design*, vol. 179, p. 103437, 2020.
- [12] J. M. Renno and B. R. Mace, "On the forced response of waveguides using the wave and finite element method," *Journal of Sound and Vibration*, vol. 329, no. 26, pp. 5474 – 5488, 2010.

- [13] Y. Waki, B. Mace, and M. Brennan, "Free and forced vibrations of a tyre using a wave/finite element approach," *Journal of Sound and Vibration*, vol. 323, no. 3, pp. 737 – 756, 2009.
- [14] R. Singh, C. Droz, M. Ichchou, F. Franco, O. Bareille, and S. De Rosa, "Stochastic wave finite element quadratic formulation for periodic media: 1D and 2D," *Mechanical Systems and Signal Processing*, vol. 136, p. 106431, 2020.
- [15] Y. Fan, C. Zhou, J. Laine, M. Ichchou, and L. Li, "Model reduction schemes for the wave and finite element method using the free modes of a unit cell," *Computers & Structures*, vol. 197, pp. 42 – 57, 2018.
- [16] J. Berenger, "A perfectly matched layer for the absorption of electromagnetic waves," *Journal of computational physics*, vol. 114, no. 2, pp. 185–200, 1994.
- [17] J. Berenger, "Three-dimensional perfectly matched layer for the absorption of electromagnetic waves," *Journal of computational physics*, vol. 127, no. 2, pp. 363–379, 1996.
- [18] F. Collino and P. Monk, "Optimizing the perfectly matched layer," *Computer methods in applied mechanics and engineering*, vol. 164, no. 1, pp. 157–171, 1998.
- [19] S. Asvadurov, V. Druskin, M. Guddati, and L. Knizhnerman, "On optimal finite-difference approximation of PML," *SIAM Journal on Numerical Analysis*, vol. 41, no. 1, pp. 287–305, 2003.
- [20] W. X. Zhong and F. W. Williams, "On the direct solution of wave propagation for repetitive structures," *Journal of Sound and Vibration*, vol. 181, no. 3, pp. 485–501, 1995.